



Interpretation of Geoelectric Pseudo Section and Seismic Refraction Tomography with Borehole Logs Carried out across a Functional Borehole at Garaje-Kagoro Area of Kaduna Northwestern Nigeria

Afuwai Gwazah Cyril

Physics Department, Kaduna State University, Kaduna PMB 2339, Kaduna State, Nigeria

Article Info

Keywords:

Borehole, Resistivity, Seismic Refraction, Garaje-Kagoro

Received 18 March 2020

Revised 05 April 2020

Accepted 06 April 2020

Available online 1 June 2020



<https://doi.org/10.37933/nipes/2.2.2020.12>

<https://nipesjournals.org.ng>
ISSN-2682-5821/© 2020 NIPES Pub.
All rights reserved

Abstract

Electrical resistivity and Seismic refraction surveys were carried out at Garaje Kagoro area of Kaduna State across a high yielding borehole to characterize the subsurface structures responsible for the high yield. Both the electrical resistivity method and the seismic refraction method show that the borehole location is underlain by four individual layers in agreement with the borehole log. The topsoil with a resistivity range of 50-140Ωm constitutes of wet brown sand and sandy clay which correlates well with the borehole log. The weathered basement which is the second layer constitutes of coarse/medium grain sand which correlates well with the borehole log. The resistivity value of the weathered basement layer ranges from 100-250Ωm. The depth to basement varies along the profile; however, averagely it is about 65m. Generally, the geophysical results revealed that the high yielding aquifer is a heterogeneous unconfined aquifer with a good yielding potential which have thick overburden deposition of fine-medium coarse grain sands. The electrical resistivity method show that the resistivity values of individual layers increases with depth. The seismic refraction method show that the velocity of individual layers increases with depth.

1. Introduction

All resistivity methods employ an artificial source of current, which is introduced into the ground through point electrodes or long line contacts. The procedure is to measure potentials at other electrodes in the vicinity of the current flow. Current is measured as well, because it is possible to determine an apparent resistivity of the subsurface. In this regard the resistivity technique is superior, at least theoretically, to all the other electrical methods because quantitative results are obtained by using a controlled source of specific dimensions. Practically, as in other geophysical methods, the maximum potentialities of resistivity are never realized. The chief drawback of the resistivity method is its high sensitivity to minor variations in conductivity of near surface. This limitation makes the resistivity method to detect more subsurface layers than the seismic refraction method. Seismic refraction maps contrast in seismic velocity i.e. the speed at which seismic energy travels through soil, rocks and other earth materials. This parameter typically correlates well with rock hardness and density which in turn tend to correlate with changes in lithology, degree of fracturing, water content and weathering. Also, there is always correlation between the topsoil thickness and depth to basement; areas where the topsoil thickness is low have low depth to basement [1].

Electrical resistivity and seismic refraction surveys were carried out at Garaje Kagoro area of Kaduna State across a high yielding borehole to characterize the subsurface structures responsible

for the high yield. The borehole at Garaje is located at latitude 8°19'53.10"E, longitude of 9°35'46.91"N and elevation of 771m. The borehole is functional. The borehole was constructed by Rural Water Supply and Sanitation Agency (WATSAN) in the year 2005; it was drilled to a depth of 60m. The recorded sufficient yield of the borehole at the point of commissioning was 15litre/min [2] which is above the minimum guideline value of 10litre/min for a successful borehole.

2. Methodology

2.1 Theory and Principle of the Electrical Resistivity Survey Method

In the DC resistivity surveying, an electric current is passed into the ground through two outer electrodes (current electrodes), and the resultant potential difference is measured across two inner electrodes (potential electrodes) that are arranged in a straight line, symmetrically about a centre point (Figure 1). The ratio of the potential difference to the current is displayed by the Terrameter as resistance. A geometric factor k in metres is calculated as a function of the electrode spacing. The electrode spacing is progressively increased, keeping the centre point of the electrode array fixed. A and B are current electrodes through which current is supplied into the ground, M and N are two potential electrodes to measure the potential differences between the two electrodes and P is the VES station to be sounded. The potential difference between the two potential electrodes is measured. The apparent resistivity is given by

$$\rho_a = k \left(\frac{\Delta V}{I} \right) \quad (1)$$

With K a geometric factor which only depends on electrode spacing and is given by:

$$K = \pi \left(\frac{L^2}{2b} - \frac{b}{2} \right) \quad (2)$$

Electrical resistivity method is defined by their frequency of operation, the origin of the source signals and the manner by which the sources and receivers are coupled to the ground. The method is generally governed by Maxwell's equations of electromagnetism. In the direct-current (DC) frequency, the diffusion term is zero and the field is thus governed entirely by Poisson equation. Electrical methods of geophysical investigations are based on the resistivity (or its inverse, conductivity) contrasts of subsurface materials. The electrical resistance, R of a material is related to its physical dimension, cross-sectional area, A and length, l through the resistivity, ρ or its inverse, conductivity, σ by:

$$\rho = \frac{1}{\sigma} = \frac{RA}{l} \quad (3)$$

Low-frequency alternating current is employed as source signals in the DC resistivity surveys in determining subsurface resistivity distributions. Thus, the magnetic properties of the materials can be ignored so that Maxwell's equations of electromagnetism reduced to:

$$\nabla \cdot \vec{E} = \frac{1}{\epsilon_0} q \quad (4)$$

$$\nabla \times \vec{E} = \mathbf{0} \quad (5)$$

Where \vec{E} is electric field in V/m , q is the charge density in C/m^3 and ϵ_0 ($8.854 \times 10^{-12} F/m$) is the permittivity of free space. These equations are applicable to continuous flow of direct current;

however, they can be used to represent the effects of alternating currents at low frequencies such that the displacement currents and induction effects are negligible. Usually, a complete homogeneous and isotropic earth medium of uniform resistivity is assumed. For a continuous current flowing in an isotropic and homogeneous medium, the current density \vec{J} is related to the electric field, \vec{E} through Ohm's law:

$$\vec{J} = \sigma \vec{E} \quad (6)$$

The electric field vector \vec{E} can be represented as the gradient of the electric scalar potential:

$$\vec{E} = \nabla \Phi \quad (7)$$

The apparent resistivity is the ratio of the potential obtained in-situ with a specific array and a specific injected current by the potential which will be obtained with the same array and current for a homogeneous and isotropic medium of $1\Omega\text{m}$ resistivity. The apparent resistivity measurements give information about resistivity for a medium whose volume is proportional to the electrode spacing [3]. Resistivity is affected more by water content and quality than the actual rock material in porous formations. While aquifers that are composed of unconsolidated materials their resistivity decreases with the degree of saturation and salinity of the groundwater [4].

The apparent resistivity is the ratio of the potential obtained in-situ with a specific array and a specific injected current by the potential which will be obtained with the same array and current for a homogeneous and isotropic medium of $1\Omega\text{m}$ resistivity. The apparent resistivity measurements give information about resistivity for a medium whose volume is proportional to the electrode spacing. Resistivity is affected more by water content and quality than the actual rock material in porous formations. Since the measured resistivity is usually a composite of the resistivity of several layers, the apparent resistivity may be smaller or larger than the real resistivities or in rare cases identical with one of the two resistivity values in a homogeneous surface. The apparent resistivity is the same as the real resistivity in a homogeneous subsurface, but normally a combination of contributing strata. The value of the apparent resistivity obtained with small electrode spacing is called the surface resistivity. Terrameter SAS300 was the primary equipment used in this study.

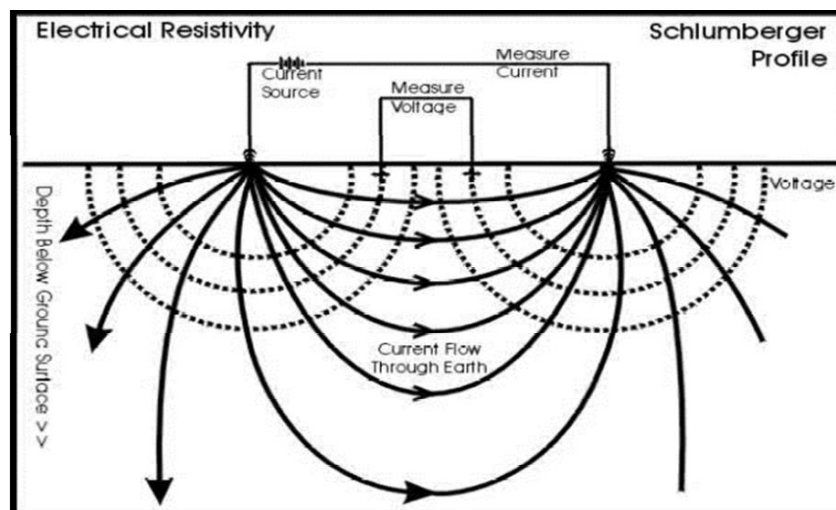


Figure 1. Schematic diagram of the schlumberger array used in the survey

A and B are current electrodes through which current is supplied into the ground, M and N are two potential electrodes to measure the potential differences between the two electrodes and P is the VES station to be sounded. The potential difference between the two potential electrode is measured.

The apparent resistivity is given by $\rho_a = K (\Delta V/I)$ with K a geometric factor which only depends on electrode spacing. The apparent resistivity is the ratio of the potential obtained in-situ with a specific array and a specific injected current by the potential which will be obtained with the same array and current for a homogeneous and isotropic medium of $1\Omega m$ resistivity. The apparent resistivity measurements give information about resistivity for a medium whose volume is proportional to the electrode spacing. Resistivity is affected more by water content and quality than the actual rock material in porous formations [5]. While aquifers that are composed of unconsolidated materials their resistivity decreases with the degree of saturation and salinity of the groundwater [6].

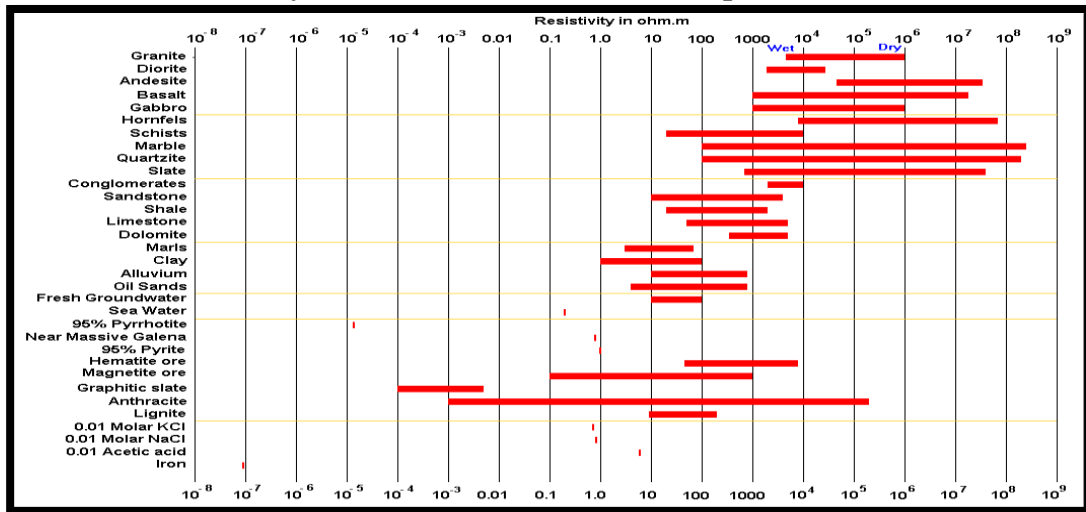
2.2 Electrical Properties of Earth Materials Adopted for the Study

Electric current flows in earth materials at shallow depths through two main methods. They are electronic conduction and electrolytic conduction. In electronic conduction, the current flow is via free electrons, such as in metals. In electrolytic conduction, the current flow is via the movement of ions in groundwater. In environmental and engineering surveys, electrolytic conduction is probably the more common mechanism. Electronic conduction is important when conductive minerals are present, such as metal sulfides and graphite in mineral surveys. The resistivity of common rocks, soil materials and chemicals [6] are shown in Table 1. Igneous and metamorphic rocks typically have high resistivity values. The resistivity of these rocks is greatly dependent on the degree of fracturing, and the percentage of the fractures filled with ground water. Thus, a given rock type can have a large range of resistivity, from about 1000 to 10 million Ωm , depending on whether it is wet or dry. This characteristic is useful in the detection of fracture zones and other weathering features, such as in engineering and groundwater surveys. Sedimentary rocks, which are usually more porous and have higher water content, normally have lower resistivity values compared to igneous and metamorphic rocks. The resistivity values range from 10 to about 10,000 Ωm , with most values below 1000 Ωm . The resistivity values are largely dependent on the porosity of the rocks, and the salinity of the contained water. Unconsolidated sediments generally have even lower resistivity values than sedimentary rocks, with values ranging from about 10 to less than 1000 Ωm . The resistivity value is dependent on the porosity (assuming all the pores are saturated) as well as the clay content. Clayey soil normally has a lower resistivity value than sandy soil. However, note the overlap in the resistivity values of the different classes of rocks and soils. This is because the resistivity of a particular rock or soil sample depends on a number of factors such as the porosity, the degree of water saturation and the concentration of dissolved salts. The resistivity of groundwater varies from 10 to 100 Ωm . depending on the concentration of dissolved salts. Note the low resistivity (about 0.2 Ωm) of seawater due to the relatively high salt content. This makes the resistivity method an ideal technique for mapping the saline and fresh water interface in coastal areas. One simple equation that gives the relationship between the resistivity of a porous rock and the fluid saturation factor is Archie's Law. It is applicable for certain types of rocks and sediments, particularly those that have a low clay content. The electrical conduction is assumed to be through the fluids filling the pores of the rock. Archie's Law is given by

$$\rho = a\rho_w\phi^{-m} \quad (8)$$

where ρ is the rock resistivity, ρ_w is fluid resistivity, ϕ is the porosity (fraction of the rock filled with the fluid) while a and m are two empirical parameters [7]. For most sedimentary rocks, a is about 1 while m is about 2, for sucrossive rocks e.g. clean consolidated sandstones and carbonates.

Table1. Resistivity values for earth materials adopted for this work [6]



2.3 Seismic Refraction Tomography

The geophysical method used for this study is seismic refraction and the technique is refraction tomography. Tomography is an inversion program where measurements are made of energy that has propagated through a medium and the character of the energy received is then used to infer the properties of the medium through which it propagates. According to [8] tomography is an imaging technique which generates a cross-sectional picture (a tomogram) of an object by utilizing the object's response to the non-destructive, probing energy of an external source. In this research work, seismic ray tomography, which is a form of travel time inversion used to determine lithologic velocity was used.

Seismic refraction tomography uses first arrival as input [9]. The solution involves minimization of the difference between the observed travel times and those predicted by ray tracing through an initial model. The solution is iterative and contains five steps:

- i. Picking of first arrivals.
- ii. Ray tracing through an initial estimate of the velocity model.
- iii. Segmenting ray paths into the portion contained in each cell of the velocity model.
- iv. Computing the difference between the observed and predicted travelled time for each ray and
- v. Iteratively back projecting the time differences to produce velocity model updates [10].

2.3.1 Seismic waves (Elastic waves)

Seismic waves (Elastic waves) are classified into two principal waves, known as body and surface waves. In the Seismic body waves, when stress is applied to an elastic body the corresponding strain is propagated outward as an elastic wave. There are two types of waves that are propagated within the main mass of the Earth. The first type is variously known as a dilatational, longitudinal, irrotational, compressional or P wave, the latter name being due to the fact that this type is usually the first (primary) event on an earthquake recording. The second type is referred to as shear, transverse, rotational or S wave (since it is usually the second event observed on earthquake record).

In compressional waves the particles of the medium move in the direction of the wave travel. The compressional waves are the fastest of all seismic waves, when an earthquake or explosion occurs; this wave is the first to arrive at a recording station. As a result, it is called a primary wave, or P wave [8]. The compressional (or longitudinal) body wave passes through a medium as a series of

dilatations and compressions. The equation of the velocity of the compressional wave is given by this relationship in Equations 9 and 10.

$$V_p = \sqrt{\left\{k + \frac{4\mu}{3}\right\}} \quad (9)$$

$$V_p = \sqrt{\frac{(1-\sigma)\epsilon}{(1+\sigma)(1-2\sigma)\rho}} \quad (10)$$

where σ is the measure of stress, k is bulk modulus and ρ is the density of medium.

For shear or S-wave, the motion of particles of the wave is perpendicular (transverse) to the direction of the wave travel. The particles of a body vibrate in a direction of the wave in transverse waves. The equation of the velocity of the shear wave is given by the relationship in Equations 11 and 12.

$$V_s = \sqrt{\frac{\mu}{\rho}} \quad (11)$$

$$V_s = \sqrt{\frac{\epsilon}{2\rho(1+\sigma)}} \quad (12)$$

The quantities λ and μ are known as Lamé constants, k , is the bulk modulus, σ is a measure of the stress and ρ , is the density of the medium. Liquids and gases do not allow shear waves to propagate through them. Consequently $\mu = 0$, and compressional wave velocity in a fluid is given by:

$$V_s = \sqrt{\frac{k}{\rho}} \quad (13)$$

The only elastic property that determines the velocity of shear waves is the rigidity or shear modulus. In liquids and gases μ is equal to zero and shear waves cannot propagate in them [10].

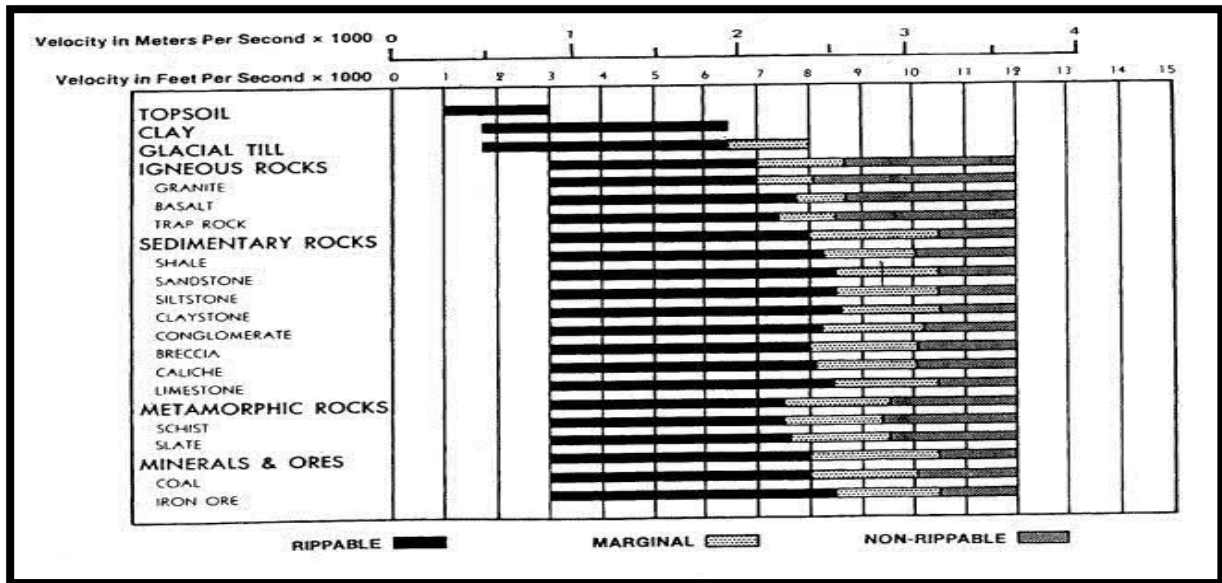
Seismic surface waves, just as the body waves, can be classified into two types: Rayleigh waves and Love waves, which are distinguished from each other by the type of particles motion in their wave fronts.

2.4 Data Collection and Processing in Seismic Refraction Tomography

The field procedure involves laying out the spread with the shot and the receivers in a straight line. The receivers are placed at an interval of 5m, which resulted in a total spread length of 120m for twenty four vertical geophones. Shots were fired at the beginning and at the end of the profile, and at each receiver point. The seismic signals generated are properly recorded with the digital seismograph. In this work a 24-channel Seistronix RAS-24 seismograph was used with a sledge hammer striking a rubber plate as an energy source and a shot-point at each geophone position. Data were stacked at least four times for each shot. Throughout the survey the geophones were placed at an interval of 5m along profile. The profile was deliberately taken across borehole location. The software ReflexW developed by [11], was used to perform the data processing and to interpret the seismic refraction tomography data. The data collected from the field was subjected to different stages of processing to enhance the signal-to-noise ratio. The data was first filtered by applying a band pass filter (with an upper and lower frequency of 150Hz and 50Hz respectively) to improve

the quality of the real signal. First-arrival travel times were picked manually and ray paths were calculated by the ray tracing method based on Huygen's principle [12].

Table2. P-wave velocity of earth materials [13].



3. Geology of the Survey Area

Garaje is located at latitude 8°19'53.1"E - 8°20'51.11"E, longitude of 9°35'46.91"N - 9°50'47.31"N at Kaura area of Kaduna state. The area is fairly flat (topographically) and located 4km at the western part of the Kagoro hill (Figure 1). Garaje and its environs are made up of mostly Newer Basalts, and rocks of the Migmatite-Gneiss Complex and Older Granites [13]. Basement rocks that occur in the study area could be classified into; Newer Basalts, Older Granites, Undifferentiated Schists and Migmatites-Gneiss Complex (Figure2).

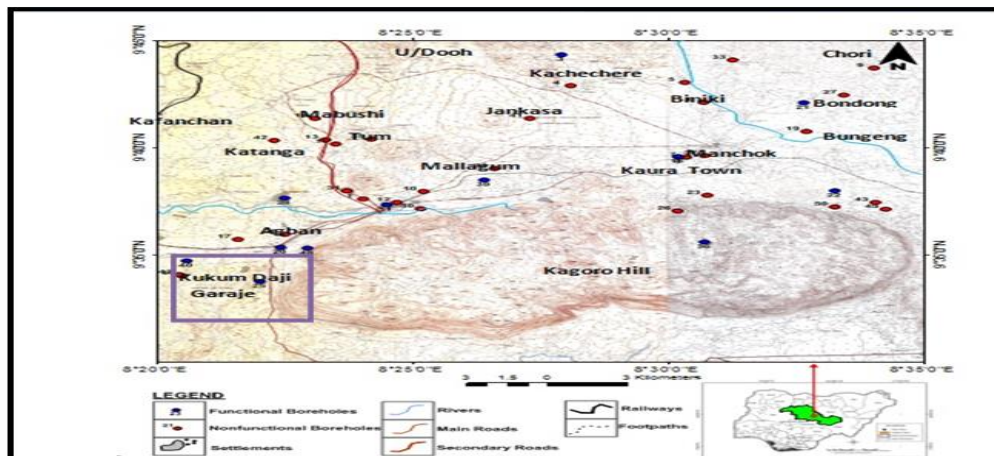
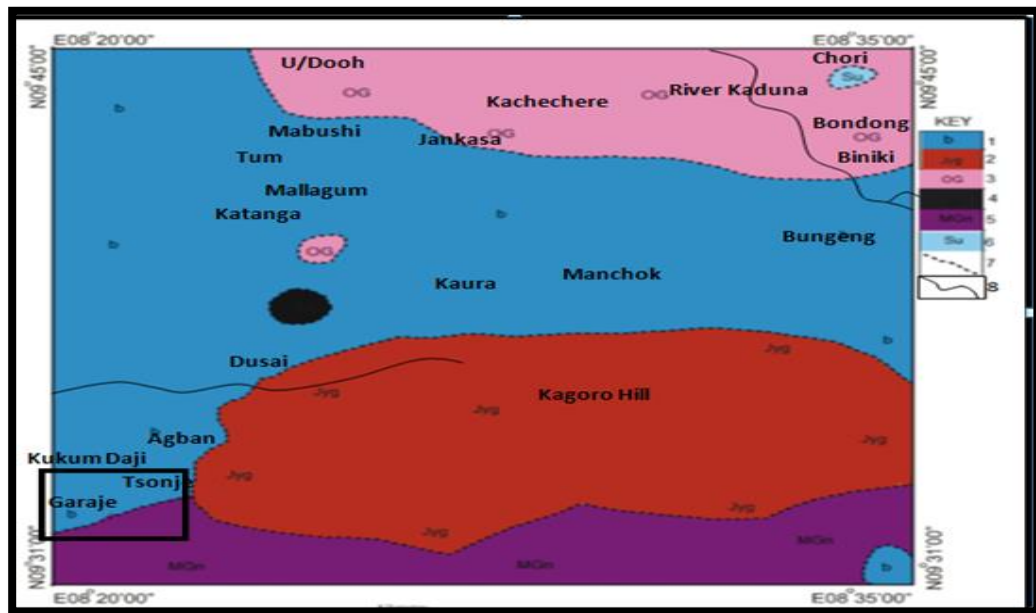


Figure2. Survey Area



1. Newer basalts 2. Younger granites 3. Older granites 4. Gneisses 5. Migmatite-Gneisses 6. Undifferentiated Schists 7. Geologic boundary
 8. River

Figure 3. Geological Map of the Kaura Area showing Garaje.

The research project was conducted at Government Secondary School Narayi, Kaduna State. The coordinates of the study area: Latitude $10^{\circ}28.275'N$ - $10^{\circ}29.15'N$ and Longitude $07^{\circ}28.649'E$ - $07^{\circ}29.14'E$. The specific location where the survey was done is an open field within the school premises. Students and other local football team play football at the study area.

4. Results and Discussion

4.1 Resistivity Pseudo Section for Garaje Profile

The pseudo section shows that along the profile which was taken along the North-South direction where the borehole is located is an aquifer with thickness of approximately 42m at a depth of 60m (Figure 4). The topsoil with a resistivity range of $50-140\Omega m$ constitutes of wet brown sand and sandy clay which correlates well with the borehole log. The weathered basement which is the second layer constitutes of coarse/medium grain sand which correlates well with the borehole log. The third layer which is taken to be the fractured layer has resistivity range of $300-400\Omega m$. The fourth layer which is the bedrock at an average depth of 65m is a fresh porphyritic granitic rock of resistivity value of $1500\Omega m$. Generally, the geophysical results revealed that the high yielding aquifer is a heterogeneous unconfined aquifer with a good yielding potential which have thick overburden deposition of fine-medium coarse grain sands.

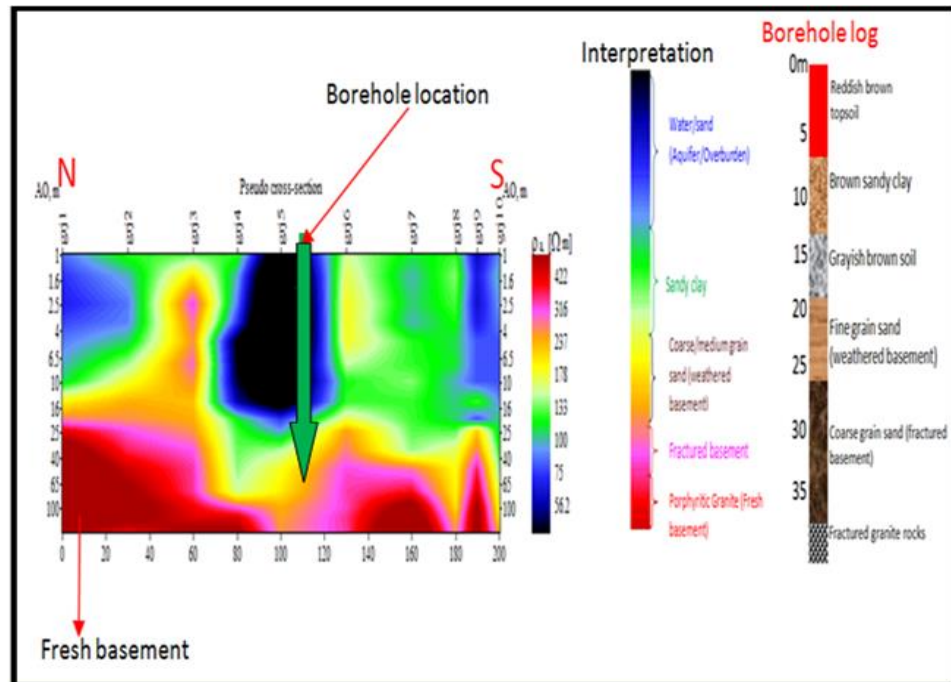


Figure 4: Geoelectric section for Garaje Profile

4.2 Seismic Refraction Tomography for Garaje Profile

The borehole at Garaje is functional. The profile was taken in the N-S azimuth directly across the borehole location. The seismic results suggest that towards the N-end, the depth to basement is lowest at a depth of 25m. The tomogram (Figure 5) shows that at depths of <8m, at the northern part of the profile, p-wave velocity range is about 250-700m/s. This range shows an obvious contrast with the p-wave velocity range of 250-2700m/s at the same depth range (<8m) at the southern part of the profile. This implies that these two sides of the profile length have soil consolidation contrast which may mean that there is discontinuity in the subsurface structures along the profile. The aquiferous layer at depths range of 4-20m, where the borehole is located has high yielding potential with thick overburden deposition of weathered sand to sustain the borehole. This result agrees well with the resistivity tomography pseudo section.

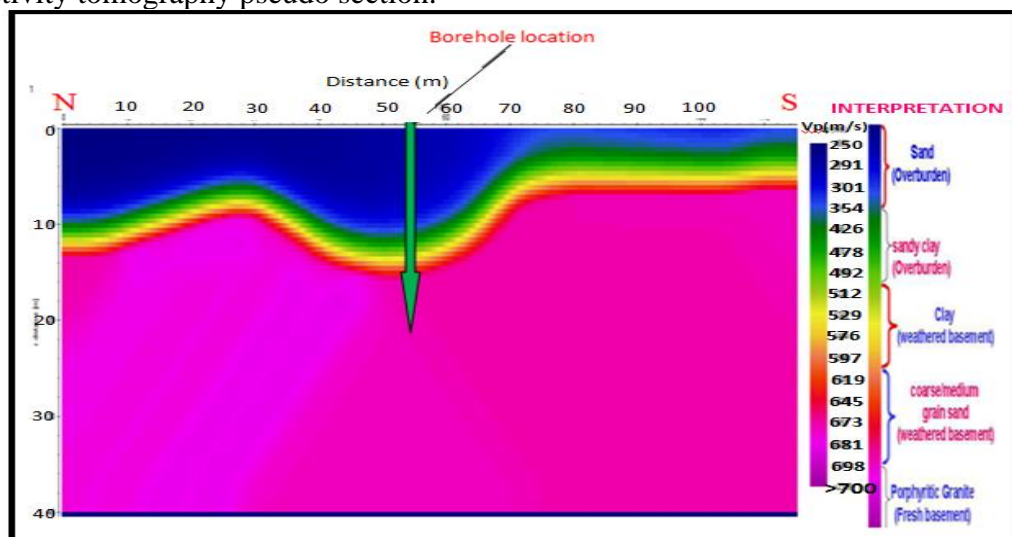


Figure 5. Seismic refraction tomogram of Garaje profile

5. Conclusion

At the end of this study it was found out that both the electrical resistivity method and the seismic refraction method show that the profile is underlain by four individual layers in agreement with the borehole log. Also, both the electrical resistivity method and the seismic refraction method revealed that the high yielding aquifer where the borehole was properly sited is a heterogeneous unconfined aquifer with a good yielding potential which have thick overburden deposition of fine-medium coarse grain sands. However, only the electrical resistivity method show that the resistivity values of individual layers increases with depth, while the seismic refraction method show that the velocity of individual layers increases with depth. It was noticed also that the depth to basement varies along the profile with an average depth of 65m.

References

- [1] Afuwai G. C., 2019. Investigation of the inhomogeneity of subsurface structures at various VES points at Samaru-Zaria, Northern-Nigeria. *Journal of Science and Technology Research* 1(1) 2019 pp. 55-62
- [2] Kaduna State Water board. (2006). *Draft Report on IBP Rural Water Supply*. pp 13-109.
- [3] Afuwai, G.C., Lawal, K.M., Sule, P.O., and Ikpokonte, A.E. (2014). Geophysical Investigation of the Causes of Borehole Failure in the Crystalline Basement Complex: A Case Study of Kaura Area of Kaduna State, Nigeria. *Journal of Environment and Earth Science* www.iiste.org Vol.4, (23), 2014.
- [4] Grant FS, West GF (1965). *Interpretation Theory in Applied Geophysics*. McGraw-Hill, New York.
- [5] Afuwai G.C. and Lawal K.M. (2013). Interpretation of Vertical Electrical Sounding Points around two boreholes at Samaru College of Agriculture ABU, Zaria-Nigeria. *Scholars Research Library, Archives of Physics Research*. 4(5). 49-54.
- [6] Foster, S. S. D., Chilton P. J., Moench M., Cardy F. and Schiffler M. (2000). *Groundwater in rural development*, World Bank Technical Paper No 463, The World Bank, Washington DC.
- [7] Keller, G. V. and Frisehknicht, F. C., (1966). *Electrical methods in geophysical Prospecting* pergamon Press.
- [8] Charles F. Narwold and William P. Owen (2005). Seismic refraction Analysis of landslides. *Geophysics and geology*, 31(4), pp 8-12.
- [9] Zhu, X., and McMechan, G. A. (1989). Estimation of two dimensional seismic compressional wave velocity distribution by iterative tomography imaging. *Journal of imaging system technology*. 1, 13-17.
- [10] Lowrie, W. (1997). *Fundamentals of geophysics*. Cambridge University press. Location Map Zaria, Sheet102.
- [11] Sandmeier K.J. Windows™ 9x/NT/2000/XP-program for the processing of seismic, acoustic or electromagnetic reflection, refraction and transmission data, Manual for REFLEXW 2003. 3:1-177. (available at www.sandmeier-geo.de).
- [12] Parasnis, D.S., (1997). *Principles of Applied Geophysics*, fifth ed., Chapman and Hall, London.
- [13] Kearey P., Hill I. and Brooks M. (2002). *An Introduction to Geophysical Exploration* (Ed). Tj International Ltd., Padstow, Cornwall, United Kingdom, 21-122.